THE JOURNAL OF BIOLOGICAL CHEMISTRY VOL. 287, NO. 22, pp. 17951–17962, May 25, 2012

Structural Adaptation of a Thermostable Biotin-binding Protein in a Psychrophilic Environment[S]

Received for publication, February 28, 2012, and in revised form, April 2, 2012 Published, JBC Papers in Press, April 5, 2012, DOI 10.1074/jbc.M112.357186

Amit Meir[‡], Edward A. Bayer[§], and Oded Livnah[‡1]

From the [‡]Department of Biological Chemistry, the Alexander Silverman Institute of Life Sciences, the Wolfson Centre for Applied Structural Biology, the Hebrew University of Jerusalem, Givat Ram, Jerusalem 91904, Israel and the [§]Department of Biological Chemistry, the Weizmann Institute of Science, 76100 Rehovot, Israel

Background: Search for novel avidins with reduced oligomeric state revealed an intriguing dimeric protein.
Results: Structures of shwanavidin from *Shewanella denitrificans* identified features accountable for high affinity and psychrophilic properties.
Conclusion: Phe-43 and disulfide bridge are responsible for the high affinity compensating the lack of intermonomeric interaction in tetrameric avidins.
Significance: Proteins from extremophile organisms provide excellent platforms toward the development of novel biotechnological utilizations.

Shwanavidin is an avidin-like protein from the marine proteobactrium *Shewanella denitrificans*, which exhibits an innate dimeric structure while maintaining high affinity toward biotin. A unique residue (Phe-43) from the L3,4 loop and a distinctive disulfide bridge were shown to account for the high affinity toward biotin. Phe-43 emulates the function and position of the critical intermonomeric Trp that characterizes the tetrameric avidins but is lacking in shwanavidin. The 18 copies of the apomonomer revealed distinctive snapshots of L3,4 and Phe-43, providing rare insight into loop flexibility, binding site accessibility, and psychrophilic adaptation. Nevertheless, as in all avidins, shwanavidin also displays high thermostability properties. The unique features of shwanavidin may provide a platform for the design of a long sought after monovalent form of avidin, which would be ideal for novel types of biotechnological application.

Proteins belonging to the avidin family are recognized for their remarkable affinity toward D-biotin (1). During the past 4 decades, the avidin-biotin system has been utilized extensively and has developed into an essential biotechnological tool in diverse fields of research and analysis (2, 3). Historically, the first avidin to be documented was from the egg white of chicken and other avian species (1). Later, streptavidins from a few *Streptomyces* species (4), and, more recently, isolated examples of avidin-like proteins were discovered in other prokaryotic (5–8) and eukaryotic (fungal) sources (9). Despite the sporadic but wide distribution of high affinity biotin-binding avidin-like proteins, their precise function in nature is essentially unknown.

Avidins are usually homotetrameric proteins with four biotin-binding sites, and their high affinity characteristics are closely dependent on their quaternary assembly (Fig. 1*A*). The monomeric subunit of all avidins consists of a highly similar topology comprising an eight-stranded antiparallel β-barrel. The tertrameric assembly is regarded as a dimer of dimers (10), each monomer of which forms three types of interactions defined as 1-2, 1-3, and 1-4 (11). The 1-2 interaction includes a critical tryptophan residue, located in the L7,8 loop (connecting β7 and β8), which is inserted into the biotin-binding site of an adjacent monomer and plays an important role in both high affinity biotin binding and tetrameric integrity (12–14). The dissociation of the avidins into dimers or monomers results in a dramatic decrease (7–8 orders of magnitude) in affinity toward biotin (13–15). The 1-4 interface forms the largest contact area ($\sim$1500 Å^2) with numerous intermonomeric interactions (Fig. 1*A*), whereas the 1-3 interface involves only 3–4 amino acids contributed by each monomer and exhibits the smallest intermolecular contact surface ($\sim$210 Å^2).

Another essential component for biotin binding is the L3,4 loop connecting strands β3 and β4. This loop is disordered in the apo forms of avidin and streptavidin, but becomes ordered upon biotin binding, leaving merely a small portion of the biotin carboxylate available to the solvent (11, 16). Additionally, upon biotin binding the L3,4 loop forms several polar interactions with biotin thus stabilizing its conformation (11, 16). In addition to the interactions with the L3,4 loop, there are important hydrophobic and polar interactions that accommodate the biotin molecule into the highly complementary contours of the binding site. In the tetrameric avidins the biotin ligand inhabits a hydrophobic box, formed by either 3 or 4 conserved aromatic residues, which is then sealed by the additional Trp contributed by a neighboring monomer. The biotin molecule is also stabilized by an intricate network of H-bond interactions in which its bicyclic segment and the carboxylate moiety are highly conserved throughout the avidin family (11, 17).

Biotechnological considerations have fueled the quest for additional avidin-like proteins that would exhibit divergent

[S] This article contains supplemental Table 1, Figs. 1 and 2, Experimental Procedures, and additional references.

The atomic coordinates and structure factors (codes 3SZI, 3SZH, 3SZJ, 3T2X, and 3T2W) have been deposited in the Protein Data Bank, Research Collaboratory for Structural Bioinformatics, Rutgers University, New Brunswick, NJ (http://www.rcsb.org/).

[1] To whom correspondence should be addressed. Tel.: 972-2-658-6894; Fax: 972-2-658-5793; E-mail: oded.livnah@huji.ac.il.

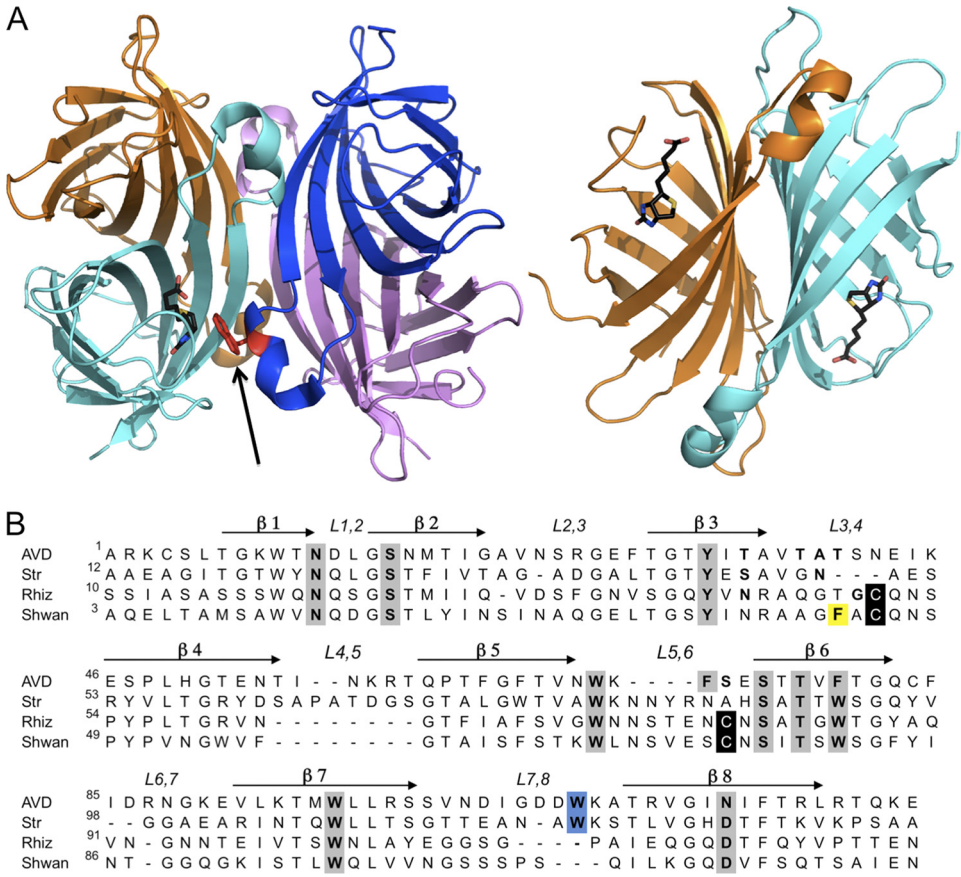

FIGURE 1. **Structures of tetrameric avidins.** *A*, tetrameric assembly of egg white avidin (*left*), with respective monomers shown in *magenta*, *blue*, *cyan*, and *orange*. The biotin ligand is shown in *black* in the binding site of the *cyan* monomer (for clarity). The Trp residue (shown in *red*) from an adjacent monomer (*blue*) contributes to the high affinity of biotin binding and is indicated by an *arrow*. The 1-4 sandwich-like monomer-monomer interaction (*right*) forms numerous stabilizing interactions (*orange* and *cyan*). All molecular graphics figures were generated using PyMOL (47). *B*, multiple sequence alignment of avidin (*AVD*), streptavidin (*Str*), rhizavidin (*Rhiz*), and shwanavidin (*Shwan*). The eight *β*-strands forming the tertiary structure are indicated by *arrows*, and the loops connecting the strands are labeled. Residues participating in biotin binding are highlighted in *gray*, cysteines participating in the disulfide bridge in the new binding site are in *black*, and the Trp residues from the L7,8 contributing to the biotin binding in tetrameric avidins are highlighted in *blue*. Phe-43 from the L3,4 loop compensates for the lack of the intermonomeric Trp residue and is highlighted in *yellow*. Shwanavidin exhibits 46, 50, and 61% sequence similarity and 26, 33, and 47% identity compared with avidin, streptavidin, and rhizavidin, respectively.

oligomeric states that could lead to the development of high affinity mono- and divalent avidins of smaller size consisting of a single polypeptide chain (18). Several attempts have been conducted to achieve these types of avidin, such as dual-chain and circular permutated avidins and streptavidins; yet, the resulting affinity of the product was compromised (19–22). In addition, a monovalent tetrameric assembly of streptavidin was obtained with one biotin-binding site available, yet its overall size remained as large as other tetrameric avidins (23).

The recently discovered rhizavidin from *Rhizobium etli* is the first known dimeric member of the avidin family (1-4 interaction) (6). The divalent form maintains high affinity toward biotin, thus providing an initial molecular platform toward the development of a minimized high affinity avidin. The 1-2 and 1-3 monomer-monomer interactions are lacking in rhizavidin, and the crucial Trp from the L7,8 loop is redundant and missing in the sequence (12, 13, 24). The crystal structure of rhizavidin provided indications of how the high affinity is maintained in the absence of the critical Trp residue (6, 25). In this context, a disulfide bridge connecting L3,4 and L5,6 contributes to the rigidity of the loops and also forms interactions with biotin; thus, the bridge was assumed to contribute to the high affinity (25).

Rhizavidin is the first member of the avidin family found to have a unique dimeric structure. We were thus interested to discover additional dimeric (or preferably monomeric) forms of avidin, to identify the diverse features contributing to the high affinity that could be further utilized to form high affinity biotin-binding monomers. In the advent of recent genome-sequencing efforts, several novel avidin-like genes have been detected, particularly in various bacteria, that could potentially exhibit high affinity biotin-binding properties. One of these sequences, identified from the Gram-negative bacterium *Shewanella denitrificans* (26), is termed herein shwanavidin. Whereas rhizavidin from *R. etli* and streptavidin from *Streptomyces avidinii* inhabit the soil rhizosphere (27), *S. denitrificans* is found at 120–130 m depths of the Baltic Sea at low temperatures (28), and shwanavidin exhibits a high degree of sequence similarity to other avidins (Fig. 1*B*). Interestingly, the protein was shown to be expressed in the parent bacterium.[2]

[2] A. Meir and O. Livnah, unpublished data.

Because shwanavidin and rhizavidin appear to form a unique subgroup in the avidin family, we aimed to determine its biochemical and structural properties. Indeed, similar to rhizavidin, shwanavidin was found to be a thermostable dimer in solution, maintaining high affinity toward biotin. However, the crystal structure of shwanavidin in the apo- and biotin-complexed forms revealed a unique feature in the binding site that contributes to the high affinity and differs significantly from that of rhizavidin. The roles of the disulfide bridge and Phe-43 in biotin binding were examined via mutagenesis and structural analysis and were found to be critical in maintaining the high affinity. Intriguingly, despite its thermostable properties, shwanavidin maintains its high affinity biotin-binding function under psychrophilic conditions. The repulsive interactions of the unique Phe-43 residue with solvent results in high flexibility of a segment of the L3,4 loop, thereby permitting biotin binding at low temperatures.

EXPERIMENTAL PROCEDURES

Shwanavidin Gene and Plasmid Construction—The shwanavidin sequence was discovered using BLAST in the UniProtKB data base via the ExPASy web site (29) as well as the NCBI BLASTp (30, 31). Shwanavidin exhibits 50 and 61% sequence similarity, 33 and 47% identity compared with streptavidin and rhizavidin, respectively. Running the BLASTn (30, 31) search with shwanavidin gene sequence *versus* the NCBI data base (32) did not result in any significant hits, not even for other *Shewanella* species. The full-length shwanavidin sequence contained 172 amino acids, where the first 42 residues were assumed to be part of a signal peptide. The last 10 residues, which also corresponds to the streptavidin C-terminal cleavage and rhizavidin flexible C′ terminus, were omitted from the synthetic gene leaving only 122 residues (residues number 43–162 from the original sequence, with 2 additional residues (Met-Ala) at the N′ terminus, resulting from two restriction sites now numbered 1–122). A synthetic gene of shwanavidin was constructed based on its amino acid sequence as available in the UniProtKB data base with codon usage suitable for *Escherichia coli* expression (by GenScript). The shwanavidin gene was cloned into a pHis2 parallel plasmid (33) using restriction enzymes NdeI and XhoI to obtain a core protein consisting of residues 43–162 with Met-Ala at the N terminus (referred to henceforth as shwanavidin). Furthermore, a His-tagged protein (His-shwanavidin), with an additional 24 residues at the N′ terminus, comprising the His_6 tag and a tobacco etch virus protease cleavage site between the His_6 and the core protein, was cloned into the vector using restriction sites NcoI and XhoI.

C45A/C74A and F43A Mutations—Site-directed mutagenesis of C45A/C74A and F43A mutants were carried out using the QuikChange kit with *Pfu* ultra DNA polymerase (Stratagene). The reaction was performed on the shwanavidin gene subcloned into pHis2 parallel (33) downstream and in-frame to the His_6-tobacco etch virus protease cleavage site coding sequence. The procedure included PCR using specific complementary primers (supplemental Table 1) followed by a DpnI digestion. The elongation step was set to 12 min at 68 °C.

Structure Determination of Shwanavidin—Expression, purification, crystallization, and data collection of shwanavidin (wild type and mutants) are described in supplemental Experimental Procedures. The native apo structure was solved by molecular replacement using PHASER (34, 35) implemented in the CCP4i suite (36). The search models included monomer and dimer from a Swiss-Model (37, 38) homology model of shwanavidin based on the rhizavidin structure (25). Matthew's coefficient indicated the presence of 8–14 shwanavidin molecules in the asymmetric unit (V_m = 2.84–1.89 Å^3/Da, 56.7–35% solvent content). The resulting PHASER solution at the resolution range of 50.0–3.0 Å using a dimeric model resulted in a dodecamer in the asymmetric unit (V_m = 1.89 Å^3/Da; 35% solvent). The structure was initially refined using the rigid body protocol in REFMAC (39) resulting in an R values of 39.7% and R_{free} of 40.1%. The structure was further refined to the resolution of 50–1.45 Å using REFMAC5, and solvent molecules were added utilizing ARP/wARP (40), after several iterative cycles of refinement and model building utilizing COOT (41) (Table 1).

Another data set of a different crystal form of apo-shwanavidin was collected to the maximal resolution of 1.07 Å (termed Form-B). The structure of the Form-B triclinic shwanavidin was solved by PHASER using the shwanavidin refined Form-A dimer as the search model at the resolution range of 50–3.5 Å. The solution indicated the presence of six shwanavidin monomers in the asymmetric unit having a V_m value of 1.96 Å^3/Da with 37.2% solvent content. The structure was refined in a similar protocol described for the Form-A apo-shwanavidin (Table 1). Crystals of the shwanavidin-biotin complex belonged to the orthorhombic space group $P2_12_12_1$ with cell parameters a = 47.7 Å, b = 56.0 Å, c = 86.6 Å. The structure of the biotin complex was solved by PHASER (50–4 Å) using the shwanavidin refined monomer as the search model. The solution indicated the presence of two shwanavidin monomers in asymmetric unit (V_m = 1.99 Å^3/Da, 35% solvent). Difference electron density maps clearly indicated the presence of biotin molecules in the corresponding binding sites.

The apo-F43A crystals belonged to the rhombohedral space group R3(H3) with cell parameters a = 113.9 Å, c = 83.4 Å, and the biotin-complex F43A crystals belonged to the tetragonal $P4_32_12$ space group; both structures were solved by PHASER using the Form-A solved structure as the search model. The solution for the apo-F43A mutant indicated the presence of four shwanavidin monomers in asymmetric unit (V_m = 2 Å^3/Da, 38.7% solvent). For the biotin complex the solution indicated one shwanavidin monomer in asymmetric unit (V_m = 1.23 Å^3/Da, 51.4% solvent). The inherent dimer was generated by a 2-fold symmetry. The difference electron density maps clearly indicated the presence of a biotin molecule in the binding site.

Affinity and Thermostability Measurements—CD spectra of the shwanavidin and its mutants were conducted using a JASCO J-810 spectrophotometer using SpectraManager software. Proteins were initially dialyzed overnight against a solution containing 10 mM NaH_2PO_4 buffer. Protein concentration was then determined using spectrophotometer, and a 7-μl saturated biotin solution was added to 200 μl of 14 μM protein solutions in 10 mM phosphate buffer and incubated for 30 min on ice. Samples with and without biotin were placed in 0.2-cm quartz cells (Starna, Atascadero, CA), and spectra were

TABLE 1
Data collection and refinement statistics

Parameter	Shwanavidin apo-Form-A	Shwanavidin apo-Form-B	Shwanavidin-biotin complex	Shwanavidin apo-F43A	Shwanavidin F43A-biotin complex
ESRF beamline	ID 23-1	ID 29	ID 23-1	ID 29	ID 29
Wavelength (Å)	0.972	0.979	0.875	0.9736	0.9736
Space group	$P2_1$	P1	$P2_12_12_1$	R3 (H3)	$P4_32_12$
Unit cell parameters (Å)	$a = 67.5$, $b = 110.6$, $c = 84.2$, $\beta = 93.9°$	$a = 43.3$, $b = 63.5$, $c = 67.7$, $\alpha = 103.8°$, $\beta = 107.3°$, $\gamma = 103.8°$	$a = 47.7$, $b = 56.0$, $c = 86.6$	$a = 113.93$, $c = 83.43$	$a = 63.21$, $c = 65.83$
Resolution range[a] (Å) (last resolution shell)	50–1.40 (1.42–1.40)	50.0–1.07 (1.09–1.07)	50.0–1.45 (1.48–1.45)	50–1.15 (1.17–1.15)	50.0–1.5 (1.53–1.5)
Unique reflections	236,160	257,028	37,616	143,125	21,973
Redundancy	2.4	3.0	4.3	3.0	6.9
$R_{sym}(I)$[b]	3.5 (52.0)	5.8 (53.9)	8.0 (58.5)	6.6 (73.0)	5.5 (93.8)
Completeness	97.5 (95.5)	92.5 (80.5)	99.8 (99.8)	99.7 (99.9)	99.2 (99.9)
I/σ	24.9 (1.6)	35.3 (1.5)	16.7 (1.5)	25.8 (1.8)	40.5 (2.15)
Number of protein atoms	11,029	5,513	1,890	3,678	890
Number of ligand atoms			32		16
Number of solvent/formate atoms	1,374/33	851	197	546	109
R factor	0.158	0.161	0.162	0.146	0.18
R_{free}[c]	0.193	0.187	0.190	0.171	0.212
Average B factor (Å^2)					
Protein	16.7	13.9	10.8	12.04	24.08
Biotin			8.6		10.58
Solvent	31.6	29.7	27.8	28.83	37.62
Formate	30.5				
R.m.s.d. from ideal					
Bond length	0.011	0.010	0.012	0.012	0.014
Bond angle	1.43	1.38	1.55	1.54	1.603
Ramachandran plot (PROCHECK) (%)					
Favored	87.8	87.0	87.8	87.9	88.8
Allowed	12.2	12.8	12.2	12.1	11.2
Generously allowed	0.0	0.2	0.0	0.0	0.0
Disallowed	0.0	0.0	0.0	0.0	0.0

[a] Outer shell resolution range.
[b] $R_{sym}(I) = \Sigma \mid I - \langle I \rangle \mid / \Sigma I$.
[c] Test set consists of 5% for all data.

recorded in the wavelength range $\lambda = 190–260$ nm, with five accumulations for each measurement and a data pitch of 0.1 nm. Background CD spectra of the appropriate buffer (with and without biotin) were recorded and subtracted from each spectrum. Thermal melts were performed by measuring CD spectra at the temperature range of 4–95 °C with a heating rate of 60 °C/h. CD signal was recorded every 0.1 °C, and the CD spectrometer was set to operate with a spectral bandwidth of 1 nm and a response time of 1 s.

The CD melting curve was measured at the wavelength of 233 nm (apo forms) and 234 nm (biotin-complex forms) where a maximum difference between the native and unfolded forms appeared. Melting temperatures (T_m) were calculated using Origin 8.1 software. Normalized T_m curves of all shwanavidin forms were then fitted to the Boltzman model, and its midpoint was calculated as the T_m. For each sample, a measurement between λ values of 190 and 260 nm was measured at 20 °C upon pre- and postheating.

The melting temperatures of native shwanavidin, in the apo- and biotin-complexed forms, were analyzed by differential scanning calorimetry (DSC).[3] The experiments were performed both in the absence and presence of biotin, in a protein concentration of 1 mg/ml (76 μM), and shwanavidin-biotin (monomer) ratio of 3:1, in 50 mM sodium phosphate, 1 M NaCl, pH 7. The thermograms (25–130 °C, 0.92 °C/min) were collected with a VP-DSC calorimeter from MicroCal (Northampton, MA). Data analysis was carried out using Origin 7.0 software (MicroCal) to calculate T_m. Because the process was nonreversible, ΔH could not be calculated.

The affinity measurements of the wild-type shwanavidin toward biotin were first conducted using the isothermal titration calorimetry (ITC) method, using a VP-ITC MicroCalorimeter instrument (MicroCal). Shwanavidin was dialyzed overnight against a sodium phosphate buffer (50 mM NaH_2PO_4, 150 mM NaCl, pH 7). After dialysis, the protein was diluted to a concentration of 12 μM. D-Biotin was diluted to a 10-fold concentration using the same buffer. The measurements were conducted at 25 °C using 10-μl titration aliquots. For comparison, 8 μM rhizavidin and 5 μM streptavidin were measured against a 10-fold concentration of D-biotin at the same buffer. Another set of K_d measurements was conducted at 4 °C. Thermal titration data were fitted to a single binding site model per monomer.

The affinity of shwanavidin and its mutants toward biotin and 2-iminobiotin was measured by the surface plasmon resonance (SPR) method using a Biacore 3000 optical biosensor instrument (Biacore AB, Uppsala, Sweden). A sensor chip was prepared by activating the surface of CM5 chip (carboxymethyl dextran-derivatized surface; Biacore AB) with a mixture of 0.4 M EDC and 0.1 M *N*-hydroxysuccinimide (NHS) followed by attachment of ethylenediamine. In the resultant chip one chan-

[3] The abbreviations used are: DSC, differential scanning calorimetry; ITC, isothermal titration calorimetry; NHS, *N*-hydroxysuccinimide; r.m.s.d., root mean square deviation; SPR, surface plasmon resonance.

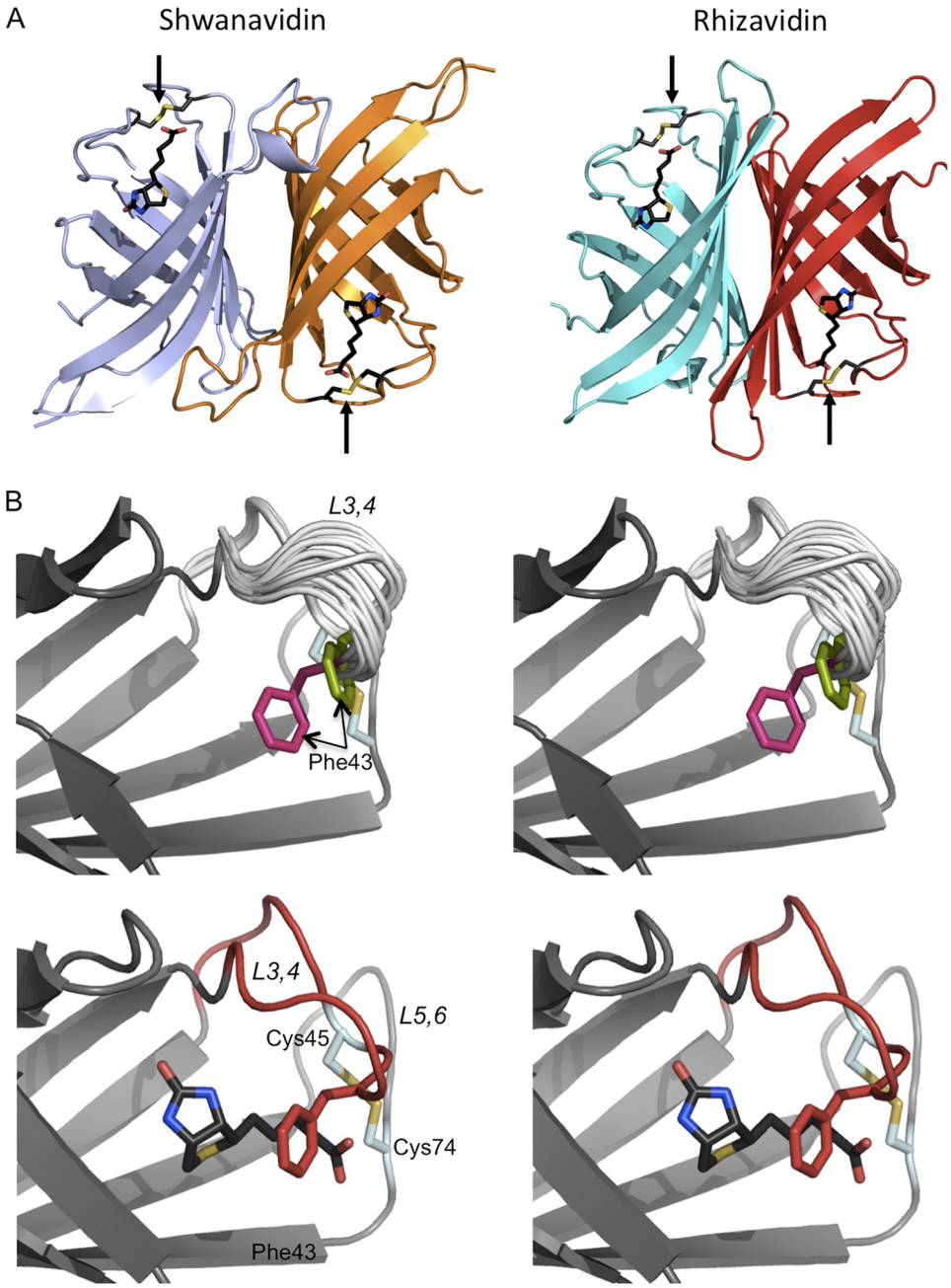

FIGURE 2. **Structure of shwanavidin.** *A*, ribbon presentations of the dimeric structures of shwanavidin (*left*) and rhizavidin (*right*) in complex with biotin (shown as *black sticks*). The two structures are very similar, forming an innate dimer consistent with the 1-4 dimeric form of the tetrameric avidins. The binding sites and the corresponding biotin (*black*) carboxylates are located at opposite positions. The disulfide bridges (colored *dark gray*, sulfurs in *yellow*) are shown in *stick* presentation indicated by *arrows*. *B*, stereo presentations of the vicinity of the biotin-binding site of apo- (*top*) and biotin-complexed (*bottom*) shwanavidin. For the apo-shwanavidin the superimposed 18 models emphasize the conformational flexibility of the L3,4 loop (*gray*) especially between residues 40 ad 44 N-terminal to the disulfide bridge. The two most extreme conformations of Phe-43 are indicated in *magenta* and *green* and indicated by *arrows*. The portion of the L3,4 loop, N-terminal to the disulfide bridge, adopts a similar conformation in all monomers; for clarity, only one conformation of the L5,6 loop is presented. In the biotin complex (biotin shown in *black*), the L3,4 loop (shown in *red*) adopts a stabilized conformation while forming hydrophobic interactions with biotin. The side chain of Phe-43 (*red*) now seals the biotin almost completely in its binding site, making most of it unavailable to solvent.

nel was treated by injecting a mixture of 0.4 M EDC and 10 mM 2-iminobiotin, and another with NHS-biotin as previously described (25). For the affinity measurements of 2-iminobiotin, 80–800 nM shwanavidin and 5–500 nM rhizavidin were injected over sensor surfaces in 1 M NaCl, 50 mM Na_2CO_3, pH 11.0 buffer. Proteins were exchanged with the buffer prior to analysis. Surfaces were regenerated between measurements by injecting 20 μl of 0.5 M acetic acid, pH 3, followed by washing with the measurement buffer. For biotin measurements, shwanavidin F43A (70 nM–2 μM), shwanavidin C45A/C74A (10–300 nM), and rhizavidin C50A/C79A (0.5–5 μM) mutants were injected over the NHS-biotin channel sensor (flow rate 20 μl/min) in 1 M NaCl, 50 mM sodium phosphate buffer, pH 7, for 240 s. Surface was regenerated between measurements by injecting 20 μl of 7.2 M urea containing 0.2 M NaOH, followed by wash with the measurement buffer for 600 s. Data analysis

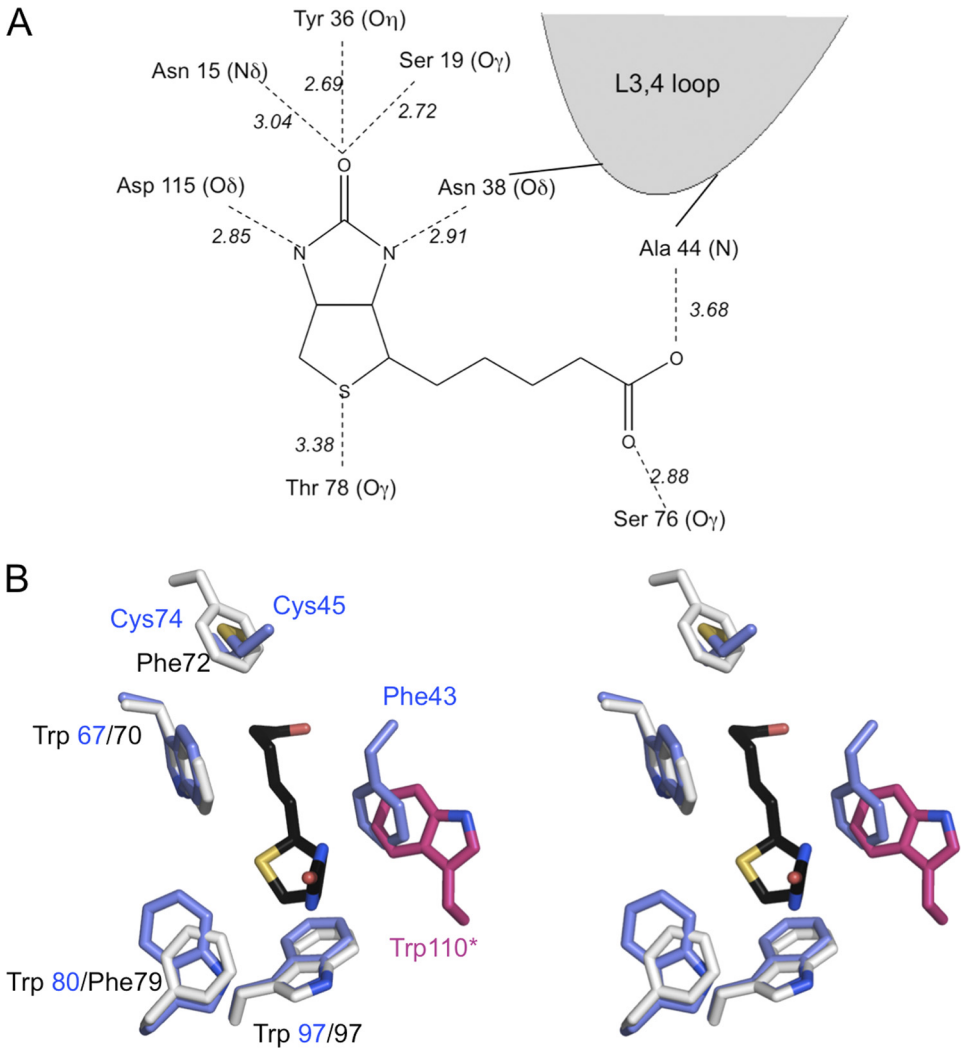

FIGURE 3. **Biotin-binding site.** *A*, schematic representation of the hydrogen-bonding network in the shwanavidin complex with biotin. The biotin ring system forms an identical network of H-bond interactions as in other avidins where five are formed with the uriedo ring and one with the tetrahydrothiophene sulfur. Furthermore, the L3,4 loop contributes a single H-bond interaction with one of the biotin ureido nitrogens. Each of the biotin carboxylate oxygens forms a single H-bond interaction with Ser-76 and main chain nitrogen of Ala-44. *B*, aromatic residues and the disulfide bridge involved in biotin binding in shwanavidin. Shown is stereo presentation of superimposed residues involved in forming the hydrophobic box accommodating biotin in shwanavidin (*light blue*) and avidin (*light gray*). For clarity, the biotin molecule (*black*) from the shwanavidin complex is shown. The disulfide bridge between the L3,4 and L5,6 loops in shwanavidin accommodates the precise position as the avidin Phe-72 side chain ring. Phe-43 from the L3,4 loop accommodates a highly similar position as Trp-110 of avidin (shown in *magenta*) contributed by an adjacent monomer. This configuration of aromatic residues in shwanavidin leaves the biotin molecule almost completely unavailable to solvent.

was performed using Biaevaluation 3.2 RC1 software, and the entire data set was fitted globally. A period of 20 s from the beginning of each injection was included in the association phase fit, and the dissociation rate analysis was performed for a 60-s period, starting immediately after the end of the injection.

A qualitative affinity assessment toward 2-iminobiotin was also conducted using an open 2-imminobiotin column. Purified shwanavidin and its F43A and C45A/C74A mutants (0.2 mg/ml) were incubated for 1.5 h with 2-iminobiotin beads (Pierce) in 50 mM sodium carbonate, 1 M NaCl buffer, pH 11, and eluted by 0.1 M acetic acid. The unbound, washed, and eluted (bound) fractions were uploaded on SDS-PAGE for analysis.

RESULTS

Structure of Shwanavidin—The resolved crystal structures reveal a molecule displaying a 1–4 dimer highly similar to that of rhizavidin (r.m.s.d. of 1.21 Å for 186 Cα pairs) (25) (Fig. 2*A* and Table 1). Gel filtration analysis clearly supported the presence of shwanavidin as a dimer in solution (supplemental Fig. 1). The inherent shwanavidin dimer is stabilized by numerous interactions with an overall contact surface area of ~1680 Å^2/monomer. As in all avidins, the tertiary structure of shwanavidin consists of an eight-antiparallel β-stranded β-barrel. A distinctive feature in shwanavidin, thus far observed only in the structure of rhizavidin, is a disulfide bridge between Cys-45 and Cys-74 linking the L3,4 and L5,6 loops, respectively. Additionally, conserved Cys residues were also found in homologous positions in sequences of other proteobacteria avidin-like proteins, whose structural characteristics have yet to be studied (5, 7, 8).

The L3,4 loop is considered to be critical for biotin binding (16, 42–44). In the apo forms of avidin and streptavidin the L3,4 loop is disordered and becomes ordered upon biotin binding by forming several polar interaction with the ligand (11, 16). In

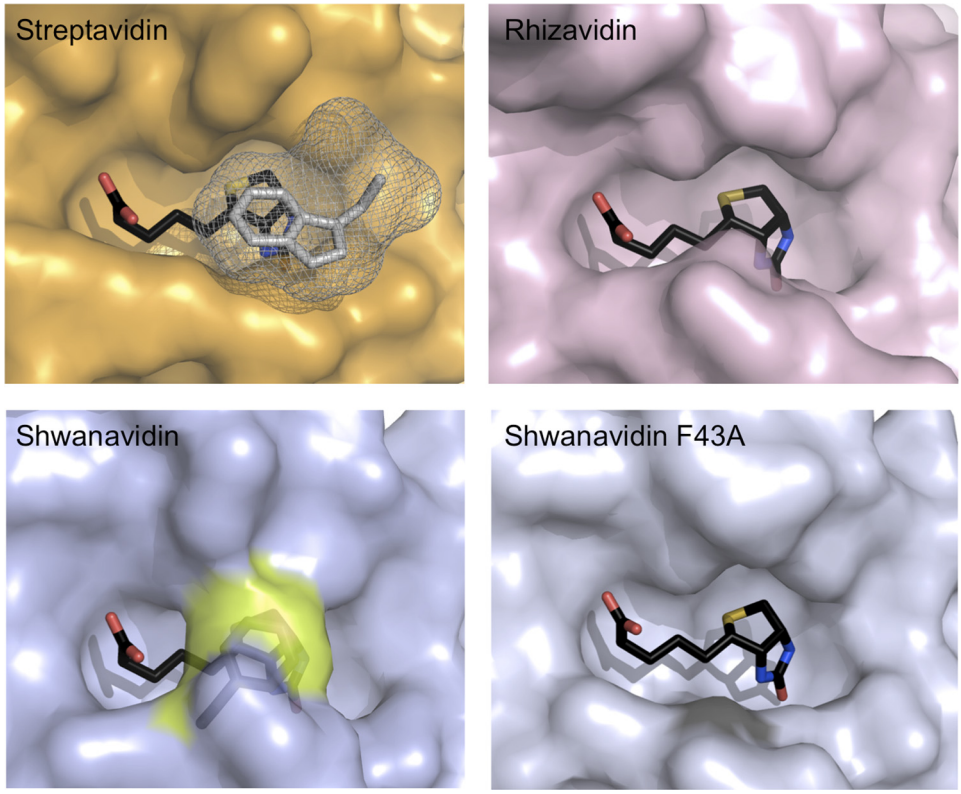

FIGURE 4. **Biotin availability in the binding sites.** Surface presentation of the biotin-complexed shwanavidin (*light blue*), rhizavidin (*light pink*), and streptavidin (*orange*) is shown. In streptavidin, the Trp-120 (shown in *gray mesh*) contributed by a neighboring monomer seals the biotin ligand almost completely. In rhizavidin and shwanavidin an equivalent Trp is lacking due to the dimeric structure. Phe-43 in shwanavidin (shown in the *transparent surface* and highlighted in *yellow*) emulates almost exactly the position of the intermonomeric Trp of the tetrameric avidins and caps the biotin molecule in the binding site, rendering the biotin molecule essentially unavailable to solvent. Upon mutating Phe-43 to Ala, the binding site of shwanavidin becomes largely exposed to solvent thus substantiating its low affinity for biotin.

TABLE 2
Affinity and thermostability properties of rhizavidin and shwanavidin

Avidin type		2-Iminobiotin K_d	Biotin K_d	T_m	
				−Biotin	+Biotin
		$\times 10^{-8}$ M	$\times 10^{-8}$ M	°C	°C
Streptavidin[a]	WT	8.5	ND[b]	75.0	112.0
Rhizavidin[c]	WT	21.5		74.8	100.5
Shwanavidin	WT	13.0		74.2	ND
				77.9 (DSC)	95.2 (DSC)
Shwanavidin	F43A		3.5	67.9	83.8
Shwanavidin	C45A/C74A		0.2	51.1	61.3
Rhizavidin	C50A/C79A		3.1		

[a] From Ref. 6.
[b] ND, not determined.
[c] From Ref. 25.

shwanavidin the L3,4 loop has the same size as avidin and rhizavidin, highly similar in composition to the latter (Fig. 1*B*). The main difference in the L3,4 between shwanavidin and rhizavidin is the presence of a Phe-43 residue rather than a Thr. For apo-shwanavidin, the A and B crystal forms provided 18 distinct copies of the monomer, which is an infrequent occurrence in crystal structure analysis (Table 1). Upon superposition of the 18 shwanavidin monomers, it is apparent that the L3,4 loop exhibits different conformational states which could represent incremental snapshots of its flexibility in solution (Fig. 2*B*). Interestingly, only about half of the loop is highly flexible. The position of Cys-45, part of the disulfide bridge, is similar in all models. In contrast, the 5 residues immediately N-terminal (residues 40–44) of Cys-45 display extremely high variability, where the maximal Cα distance between the two most extreme conformations for Phe-43 is 2.43 Å (r.m.s.d. of 2.02 Å for Cαs of residues 40–44) (Fig. 2*B*).

Biotin Binding Site—Upon biotin binding, the L3,4 loop adopts a distinct conformation while forming polar and hydrophobic interactions with biotin (Fig. 3). The polar interactions of shwanavidin with biotin consist of a canonical network of H-bond interactions largely identical in most avidins (Fig. 3). The biotin bicyclic ring forms six conserved polar interactions. The biotin ureido ring carbonyl group is stabilized by three H-bond interactions with Asn-15 Nδ, Ser-19 Oγ, and Tyr-36 Oη. The tetrahydrothiophene ring sulfur forms a polar interaction with Thr-78 Oγ. One oxygen of the biotin carboxylate moiety is stabilized by H-bond interactions with Ala-44 N,

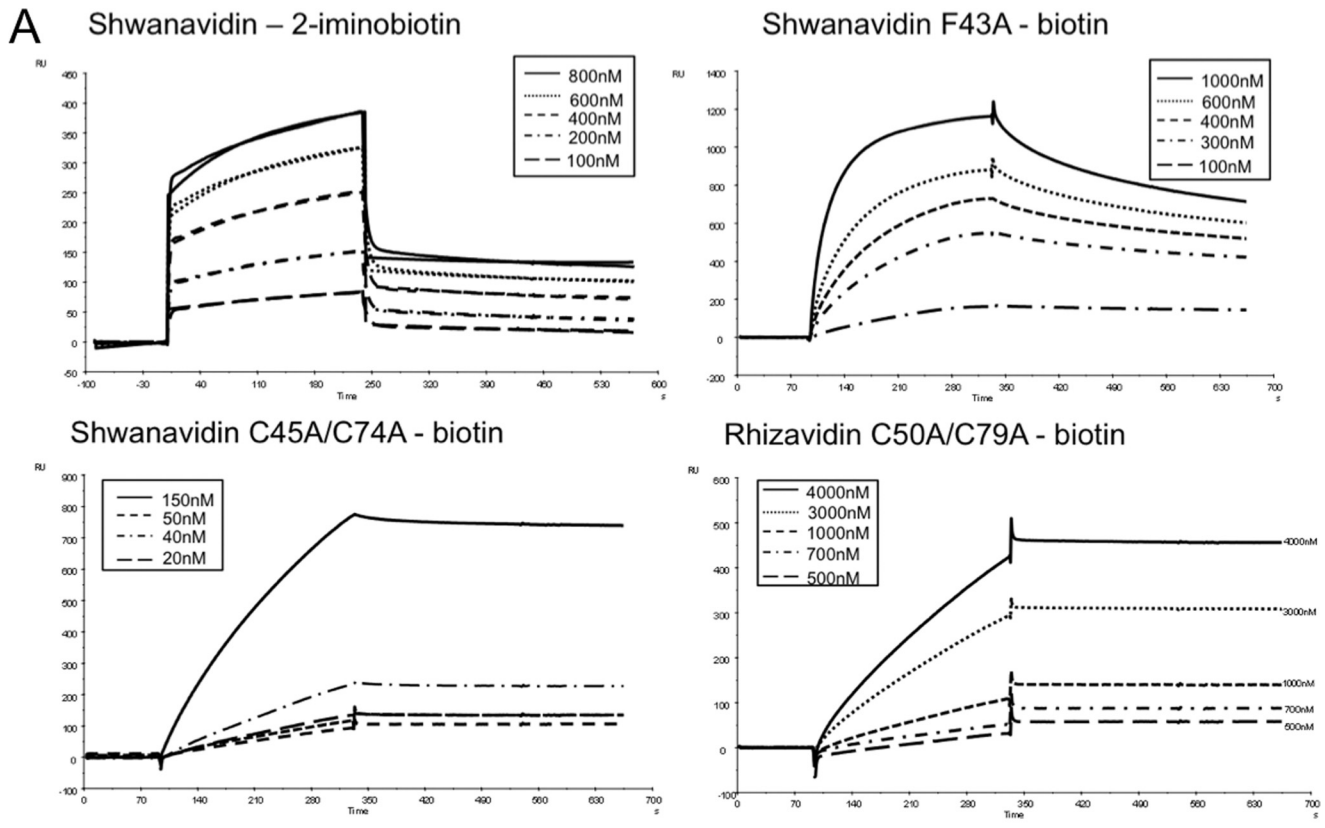
A
Shwanavidin – 2-iminobiotin
800nM
600nM
400nM
200nM
100nM
Shwanavidin F43A - biotin
1000nM
600nM
400nM
300nM
100nM
Shwanavidin C45A/C74A - biotin
150nM
50nM
40nM
20nM
Rhizavidin C50A/C79A - biotin
4000nM
3000nM
1000nM
700nM
500nM
RU
Time

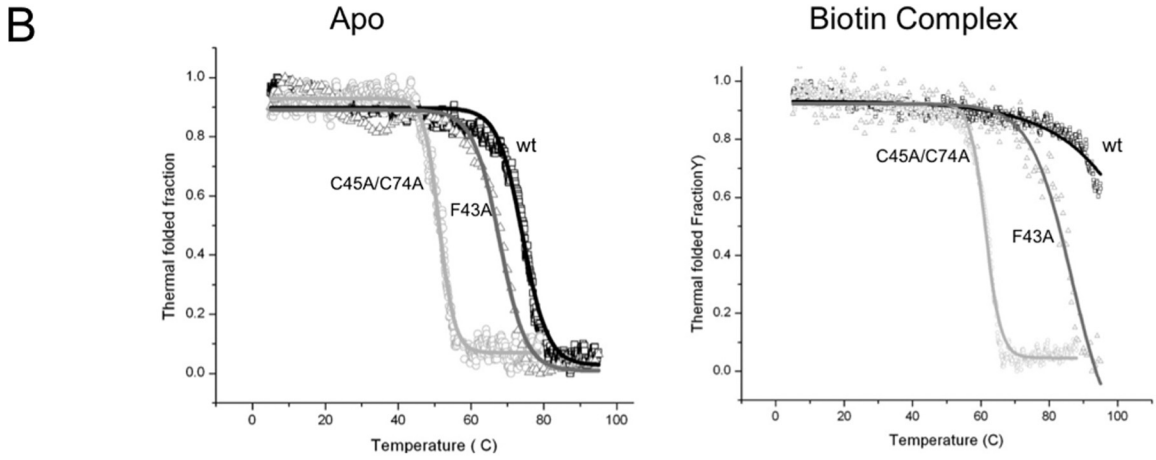
B
Apo
Biotin Complex
Thermal folded fraction
Thermal folded FractionY)
wt
C45A/C74A
F43A
Temperature (C)
Temperature (C)

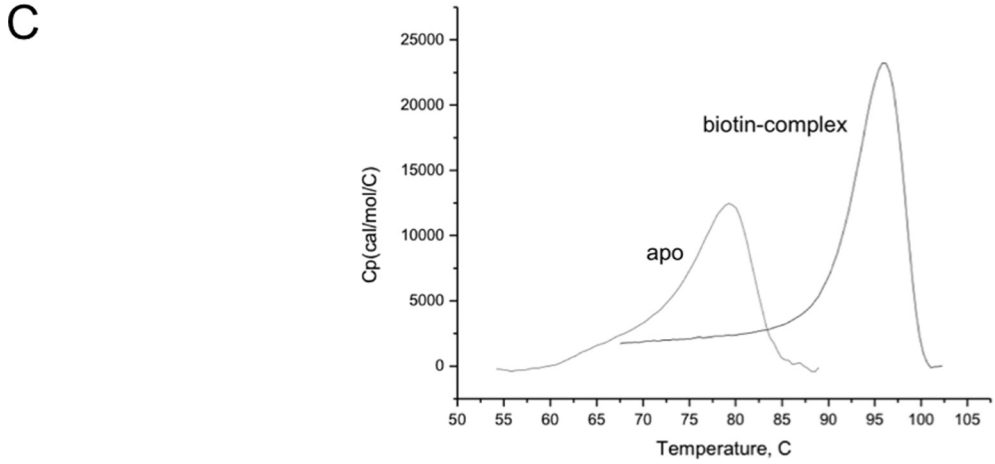
C
biotin-complex
apo
Cp(cal/mol/C)
Temperature, C

whereas the other interacts with Ser-76 Oγ. In addition to maintaining the rigidity of the L3,4 and L5,6 loops, the disulfide bridge also contributes to the stabilization of biotin in the binding site, similar to that also observed for rhizavidin. The disulfide bridge is located in a position equivalent to Phe-72 in avidin, where the latter participates in the extended hydrophobic box of the biotin-binding site (Fig. 3). The disulfide bridge is also stabilized by an H-bond interaction of Cys-45 S with Tyr-50 Oη (3.2Å), where the latter residue is conserved in all avidins exhibiting 2 Cys residues in the same positions.

In addition to the polar interactions, there are critical hydrophobic interactions consisting mainly of conserved aromatic residues forming the canonical hydrophobic box. In this regard, there are three Trp residues (Trp-67, Trp-80, and Trp-97) in shwanavidin, which are also conserved in rhizavidin (25) (Fig. 3). Unlike rhizavidin, however, there is a significant addition to the framework of the aromatic box in the binding site. The Phe-43, contributed by the L3,4 loop and unique to shwanavidin, represents an additional feature of the hydrophobic box and seals almost completely the ligand in its binding site (Fig. 4). The interaction of Phe-43 with biotin also contributes to the overall stability of the L3,4 loop. Incredibly, the uniqueness of Phe-43 is far more pronounced because its side chain is situated almost precisely where the Trp residues from L7,8 in tetrameric avidins are positioned (Figs. 3 and 4). Phe-43 thus compensates for the lack of the Trp residue and maintains a more complete configuration of the hydrophobic box compared with that of the tetrameric avidins.

Structure of F43A Mutant—To examine the role of Phe-43 in biotin binding, we mutated this residue into alanine. Biophysical studies of this mutant (see below) indicated that the resultant affinity indeed decreased substantially ($K_d \sim 10^{-8}$ M), yet the overall structural features remained remarkably similar to those of the wild-type molecule. However, there are notable differences in the L3,4 loop which affect the biotin-binding site and consequently the affinity. Unlike wild-type shwanavidin, the entire L3,4 loop region of the mutant is well ordered in the apo form. Upon biotin binding, only a small conformational change is observed in L3,4 compared with the wild-type protein. The substitution of Phe-43 by Ala leaves biotin far more available to solvent (Fig. 4). Furthermore, unlike in the wild-type shwanavidin, the distance between one of the biotin carboxylic oxygens to Ala-44 N (4.7 Å) indicates that the H-bond interactions available in the wild-type protein could not be formed (data not shown), thereby decreasing stabilization of the biotin ligand in the binding site (Fig. 4). The remaining polar and hydrophobic interactions between the protein and biotin are identical to those of the wild-type protein.

Affinity and Thermostability Characteristics of Shwanavidin—ITC measurements of the interaction between shwanavidin and biotin revealed an extremely high affinity similar to that observed for rhizavidin and streptavidin. The data were fitted to a single set of one site and resulted in a single data point for the K_a slope, indicating that the affinities exceed the capacity of this method (supplemental Fig. 2). Hence, further affinity assays were conducted using SPR as described previously for rhizavidin (25). The binding of rhizavidin to the biotin-coated chip essentially resulted in irreversible binding, even in the presence of 7.2 M urea, and affinity assays were therefore performed using 2-iminobiotin at pH 11.0 where its affinity toward the avidins is maximal. The affinity of shwanavidin toward 2-iminobiotin is of the same order of magnitude (10^{-7} M) as that reported for rhizavidin (Table 2). Both the F43A and C45A/C74A mutants were unable to bind 2-iminobiotin even at high concentrations. However, the mutants all bound biotin at lower affinities, compared with wild-type shwanavidin, with K_d values of 10^{-8} and 10^{-9} M for F43A and C45A/C74A, respectively. Similarly, the disulfide bridge mutant (C50A/C79A) of rhizavidin also exhibited decreased affinity for biotin ($K_d = 3.1 \times 10^{-8}$ M) (Fig. 5*A* and Table 2).

To assess further the affinity of the shwanavidin and rhizavidin mutants toward 2-iminobiotin, the two dimeric forms of avidin were incubated with 2-iminobiotin beads at high pH values (11). Whereas wild-type shwanavidin bound to the column and was eluted by reducing the pH, the mutants failed to bind to the resin, indicating very low affinity toward 2-iminobiotin, in agreement with the SPR results. Wild-type shwanavidin could thus be purified using a one-step protocol, whereas the mutants required a different purification strategy.

The thermal stability characteristics of shwanavidin and its mutants were initially evaluated using circular dichroism (CD). The measurements were performed on shwanavidin (wild type and mutants) in their apo- and biotin-complexed forms, using rhizavidin as a control. All samples were measured within the temperature range of 4–95 °C in 10 mM sodium phosphate buffer, pH 4.8. The T_m value for apo-shwanavidin was determined to be 74.2 °C, whereas the biotin complex remained stable to 95 °C, hence its thermostability curve could not be determined (Fig. 5*B* and Table 2). Thus, biotin has a stabilizing effect on shwanavidin, and further measurements of the apo- and biotin complex were thus performed using DSC. DSC measurements revealed the T_m of the apo- and biotin-complexed shwanavidin to be 77.9 and 95.2 °C, respectively (Fig. 5*C* and Table 2). These results are in agreement with previously reported val-

FIGURE 5. **Binding and thermostability properties.** *A*, SPR sensograms showing the association and dissociation of wild-type shwanavidin to 2-iminobiotin. Because the shwanavidin F43A mutant and the disulfide bridge mutants of shwanavidin and rhizaividin did not bind 2-iminobiotin, SPR measurements were conducted using biotin. Protein samples were injected over the chip surface for 240 s at a flow rate of 20 μl/min and then washed with elution buffer without protein for 300 s. Shwanavidin sensograms are similar to those reported previously for rhizavidin (25). The disulfide bridge mutants from shwanavidin and rhizavidin show similar sensograms, although in rhizavidin the K_d is 1 order of magnitude higher than that of shwanavidin. *RU*, response unit. *B*, CD thermograms of shwanavidin wild type and mutants (F43A and C45A/C74A). Data were normalized to the thermostable fraction, ranging between 1 (natively folded protein) and 0 (unfolded). Sigmoidal plots of the folded state *versus* temperature in λ values of 233 and 234 nm for the apo- and biotin-complexed proteins, respectively, clearly show the shift in thermostability upon mutating Phe-43 and the disulfide bridges. *C*, DSC thermograms of shwanavidin as a function of temperature measured in the absence and presence of biotin in 1 M NaCl, 50 mM NaH_2PO_4, pH 7. The T_m values of 77.2 and 95.2 °C were obtained at the highest point in the thermograms for the apo- and biotin-complexed shwanavidin, respectively, indicating a higher stability upon biotin binding.

ues for rhizavidin and other avidins (6, 45), clearly validating shwanavidin as a thermostable protein (Table 2).

The CD measurements for the shwanavidin mutants (F43A and C45A/74A) displayed a dramatic decrease in thermostability properties. For the apo-F43A mutant, a T_m value of 67.9 °C was evaluated, where the biotin-complexed protein exhibited higher stability with a T_m value of 83.8 °C. The double C45A/C74A mutant of shwanavidin had a more dramatic effect on thermal stability with T_m values of 51.1 and 61.3 °C for the apo- and biotin-complexed molecules, respectively (Fig. 5*B* and Table 2).

DISCUSSION

The search for novel avidins with unique characteristics has led us to the discovery of a bacterial sequence bearing features consistent with a high propensity to bind biotin. Shwanavidin from the marine bacterium, *S. denitrificans,* is the second known innate homodimeric avidin-like protein (after rhizavidin) which maintains high affinity toward biotin. Rhizavidin and shwanavidin are highly similar in structure and biotin-binding site, yet the latter has an exceptional structural feature, a unique Phe-43 residue located on the L3,4 loop, which emulates the precise position of the crucial intermonomeric Trp in tetrameric avidins (Figs. 3 and 4) (11, 13). The intramonomeric Phe-43 seals the biotin molecule almost completely, thus mimicking the binding-site framework in tetrameric avidins.

Intriguingly, the two crystal forms of apo-shwanavidin provide 18 copies of its monomer, which collectively provide a unique insight into the structural flexibility of residues 40–44 of the L3,4 loop. Mutating Phe-43 into alanine resulted in a striking decrease in affinity toward biotin and eliminated binding to 2-iminobiotin. In addition, the L3,4 loop in the F43A mutant is far less flexible and exhibits a similar conformation in the two subunits. Hence, the presence of solvent-exposed Phe-43 appears to be unfavorable, probably due to its repulsive interactions with solvent molecules leading to multiple conformations. Upon biotin binding, Phe-43 forms hydrophobic interactions with biotin resulting in conformational stability. Removal of Phe-43 in the F43A mutant substantially increases the availability of biotin to solvent, resulting in lower affinity for the ligand (Fig. 4 and Table 2). A similar phenomenon was observed upon mutating the analogous Trp-120 in streptavidin to Ala, whereby the affinity decreased from 10^{-14} to 10^{-7} M (46). Mutating the intermonomeric Trp into Lys in avidin and streptavidin resulted in the dissociation into dimers in solution and decreased affinity toward biotin ($\sim 10^{-8}$ M) (12).

One of the essential biotin-binding characteristics of both rhizavidin and shwanavidin is the disulfide bridge, which connects loops L3,4 and L5,6. The disulfide bridge of both proteins resides in a similar position, forming almost identical interactions with biotin (25) (Fig. 3). Its role in the high affinity biotin binding was clearly established via mutagenesis of the corresponding Cys residues into Ala. The resulting affinity toward biotin was substantially decreased for both rhizavidin and shwanavidin. Moreover, their binding capacities toward 2-iminobiotin were completely abolished. Hence, removal of the disulfide bridge likely increases the flexibility of the L3,4 and L5,6 loops and the respective degrees of freedom, resulting in a higher loss of entropy and weaker binding of biotin. The apparent increase in flexibility of the unrestrained L3,4 loop renders the bound biotin molecule more available to solvent, thus increasing the off rate of the ligand. In addition, the higher flexibility and entropy could explain the decrease in the corresponding T_m values of the mutant. The high flexibility in the L3,4 and L5,6 loops could also serve as a rationale as to why crystals of the C45A/C74A mutant could not be obtained.

The dimeric rhizavidin and shwanavidin show extremely similar characteristics in their overall structural topology and functional properties. Each originates from a different host bacterium which inhabits a distinctive environment. Whereas rhizavidin from *R. etli* is found in the soil rhizosphere habitat (27), shwanavidin is found in the deep Gotland basin region of the Baltic Sea, at a depth of 120–130 m (26). Furthermore, both rhizavidin and shwanavidin are unique proteins in their families, where no other species of *Shewanella* or *Rhizobium* is known to exhibit another avidin-like sequence in its genome. If ancestral forms of the two bacteria occupied the same environment, acquisition of these avidin-like molecules could reflect horizontal gene transfer event(s). However, because the environments are so distinct and different, other explanations such as convergent or divergent evolution resulting in environmental adaptation could also be possible. In this regard, shwanavidin might have gone through adaptive changes for the low temperature environment. Psychrophilic proteins are reported to have a higher ligand-accessible binding site compared with their mesophilic homologs (48). Flexible loops in the vicinity of the ligand-binding site are one way to increase its availability. Hence, the presence of solvent-exposed Phe-43 in the L3,4 loop results in entropic destabilization of the 40–44 segment of the loop. The observed flexibility in the loop increases the availability of the binding site to the ligand (49) (Fig. 2). After biotin binding, the loop forms stabilizing interactions with biotin, thus adopting a defined conformation. The presence of Phe-43 could thus reflect adaptation to the cold environment of shwanavidin while maintaining its function (48).

Natural evolutionary adaptations of avidin-like proteins have revealed many of the subtle molecular determinants that generated high affinity biotin-binding properties in their dimeric forms. Together with rhizavidin, the high affinity of dimeric shwanavidin provides an excellent platform toward the design of monovalent high affinity biotin-binding systems. Moreover, continued searches of the expanding genomic data bases could also lead to the discovery of a monomeric homolog that maintains high affinity toward biotin. The adaptability of the thermostable shwanavidin into a cold environment also extends its potential utilization in biotechnological applications over a large temperature range.

Accession Codes—The coordinates and the corresponding structure factors of the solved structure are available in the RCSB-PDB data base with the entry codes of 3SZI, 3SZH, 3SZJ, 3T2X, 3T2W, for the shwanavidin apo-form A, form B, biotin complex, apo-F43A, and F43A biotin complex, respectively.

Acknowledgments—We thank Prof. Manfred Höfle, Helmholtz Centre for Infection Research, Braunschweig, Germany, for providing the S. denitrificans strain OS217; the staff of ESRF for upgrading and maintaining the first class facility; Shahar Sukenik for assistance with the CD measurements; and Dr. Aharon Rabinkof and Dr. Irina Shin for assistance in conducting the SPR, ITC, and DSC measurements.

REFERENCES

1. Green, N. M. (1975) Avidin. *Adv. Protein Chem.* **29,** 85–133
2. Wilchek, M., and Bayer, E. A. (1989) Avidin-biotin technology ten years on: has it lived up to its expectations? *Trends Biochem. Sci.* **14,** 408–412
3. Bayer, E. A., and Wilchek, M. (1990) Application of avidin-biotin technology to affinity-based separations. *J. Chromatogr.* **510,** 3–11
4. Bayer, E. A., Kulik, T., Adar, R., and Wilchek, M. (1995) Close similarity among streptavidin-like, biotin-binding proteins from *Streptomyces*. *Biochim. Biophys. Acta* **1263,** 60–66
5. Helppolainen, S. H., Määttä, J. A., Halling, K. K., Slotte, J. P., Hytönen, V. P., Jänis, J., Vainiotalo, P., Kulomaa, M. S., and Nordlund, H. R. (2008) Bradavidin II from *Bradyrhizobium japonicum*: a new avidin-like biotin-binding protein. *Biochim. Biophys. Acta* **1784,** 1002–1010
6. Helppolainen, S. H., Nurminen, K. P., Määttä, J. A., Halling, K. K., Slotte, J. P., Huhtala, T., Liimatainen, T., Ylä-Herttuala, S., Airenne, K. J., Närvänen, A., Jänis, J., Vainiotalo, P., Valjakka, J., Kulomaa, M. S., and Nordlund, H. R. (2007) Rhizavidin from *Rhizobium etli*: the first natural dimer in the avidin protein family. *Biochem. J.* **405,** 397–405
7. Nordlund, H. R., Hytönen, V. P., Laitinen, O. H., and Kulomaa, M. S. (2005) Novel avidin-like protein from a root nodule symbiotic bacterium, *Bradyrhizobium japonicum*. *J. Biol. Chem.* **280,** 13250–13255
8. Sardo, A., Wohlschlager, T., Lo, C., Zoller, H., Ward, T. R., and Creus, M. (2011) Burkavidin: a novel secreted biotin-binding protein from the human pathogen *Burkholderia pseudomallei*. *Protein Expr. Purif.* **77,** 131–139
9. Takakura, Y., Tsunashima, M., Suzuki, J., Usami, S., Kakuta, Y., Okino, N., Ito, M., and Yamamoto, T. (2009) Tamavidins: novel avidin-like biotin-binding proteins from the tamogitake mushroom. *FEBS J.* **276,** 1383–1397
10. Kurzban, G. P., Bayer, E. A., Wilchek, M., and Horowitz, P. M. (1991) The quaternary structure of streptavidin in urea. *J. Biol. Chem.* **266,** 14470–14477
11. Livnah, O., Bayer, E. A., Wilchek, M., and Sussman, J. L. (1993) Three-dimensional structures of avidin and the avidin-biotin complex. *Proc. Natl. Acad. Sci. U.S.A.* **90,** 5076–5080
12. Laitinen, O. H., Airenne, K. J., Marttila, A. T., Kulik, T., Porkka, E., Bayer, E. A., Wilchek, M., and Kulomaa, M. S. (1999) Mutation of a critical tryptophan to lysine in avidin or streptavidin may explain why sea urchin fibropellin adopts an avidin-like domain. *FEBS Lett.* **461,** 52–58
13. Freitag, S., Le Trong, I., Chilkoti, A., Klumb, L. A., Stayton, P. S., and Stenkamp, R. E. (1998) Structural studies of binding site tryptophan mutants in the high affinity streptavidin-biotin complex. *J. Mol. Biol.* **279,** 211–221
14. Sano, T., Vajda, S., Smith, C. L., and Cantor, C. R. (1997) Engineering subunit association of multisubunit proteins: a dimeric streptavidin. *Proc. Natl. Acad. Sci. U.S.A.* **94,** 6153–6158
15. Pazy, Y., Eisenberg-Domovich, Y., Laitinen, O. H., Kulomaa, M. S., Bayer, E. A., Wilchek, M., and Livnah, O. (2003) Dimer-tetramer transition between solution and crystalline states of streptavidin and avidin mutants. *J. Bacteriol.* **185,** 4050–4056
16. Weber, P. C., Ohlendorf, D. H., Wendoloski, J. J., and Salemme, F. R. (1989) Structural origins of high affinity biotin binding to streptavidin. *Science* **243,** 85–88
17. Eisenberg-Domovich, Y., Hytönen, V. P., Wilchek, M., Bayer, E. A., Kulomaa, M. S., and Livnah, O. (2005) High-resolution crystal structure of an avidin-related protein: insight into high affinity biotin binding and protein stability. *Acta Crystallogr. D Biol. Crystallogr.* **61,** 528–538
18. Lim, K. H., Huang, H., Pralle, A., and Park, S. (2011) Engineered streptavidin monomer and dimer with improved stability and function. *Biochemistry* **50,** 8682–8691
19. Freitag, S., Le Trong, I., Klumb, L., Stayton, P. S., and Stenkamp, R. E. (1997) Structural studies of the streptavidin binding loop. *Protein Sci.* **6,** 1157–1166
20. Nordlund, H. R., Hytönen, V. P., Hörhä, J., Määttä, J. A., White, D. J., Halling, K., Porkka, E. J., Slotte, J. P., Laitinen, O. H., and Kulomaa, M. S. (2005) Tetravalent single-chain avidin: from subunits to protein domains via circularly permuted avidins. *Biochem. J.* **392,** 485–491
21. Nordlund, H. R., Laitinen, O. H., Hytönen, V. P., Uotila, S. T., Porkka, E., and Kulomaa, M. S. (2004) Construction of a dual chain pseudotetrameric chicken avidin by combining two circularly permuted avidins. *J. Biol. Chem.* **279,** 36715–36719
22. Chivers, C. E., Crozat, E., Chu, C., Moy, V. T., Sherratt, D. J., and Howarth, M. (2010) A streptavidin variant with slower biotin dissociation and increased mechanostability. *Nat. Methods* **7,** 391–393
23. Howarth, M., Chinnapen, D. J., Gerrow, K., Dorrestein, P. C., Grandy, M. R., Kelleher, N. L., El-Husseini, A., and Ting, A. Y. (2006) A monovalent streptavidin with a single femtomolar biotin binding site. *Nat. Methods* **3,** 267–273
24. Sano, T., Smith, C. L., and Cantor, C. R. (1997) Expression and purification of recombinant streptavidin-containing chimeric proteins. *Methods Mol. Biol.* **63,** 119–128
25. Meir, A., Helppolainen, S. H., Podoly, E., Nordlund, H. R., Hytönen, V. P., Määttä, J. A., Wilchek, M., Bayer, E. A., Kulomaa, M. S., and Livnah, O. (2009) Crystal structure of rhizavidin: insights into the enigmatic high-affinity interaction of an innate biotin-binding protein dimer. *J. Mol. Biol.* **386,** 379–390
26. Brettar, I., Christen, R., and Höfle, M. G. (2002) *Shewanella denitrificans* sp. nov., a vigorously denitrifying bacterium isolated from the oxic-anoxic interface of the Gotland Deep in the central Baltic Sea. *Int. J. Syst. Evol. Microbiol.* **52,** 2211–2217
27. González, V., Santamaría, R. I., Bustos, P., Hernández-González, I., Medrano-Soto, A., Moreno-Hagelsieb, G., Janga, S. C., Ramírez, M. A., Jiménez-Jacinto, V., Collado-Vides, J., and Dávila, G. (2006) The partitioned *Rhizobium etli* genome: genetic and metabolic redundancy in seven interacting replicons. *Proc. Natl. Acad. Sci. U.S.A.* **103,** 3834–3839
28. Brettar, I., Christen, R., and Höfle, M. G. (2012) Analysis of bacterial core communities in the central Baltic by comparative RNA-DNA-based fingerprinting provides links to structure-function relationships. *Isme J.* **6,** 195–212
29. Gasteiger, E., Gattiker, A., Hoogland, C., Ivanyi, I., Appel, R. D., and Bairoch, A. (2003) ExPASy: the proteomics server for in-depth protein knowledge and analysis. *Nucleic Acids Res.* **31,** 3784–3788
30. Camacho, C., Coulouris, G., Avagyan, V., Ma, N., Papadopoulos, J., Bealer, K., and Madden, T. L. (2009) BLAST+: architecture and applications. *BMC Bioinformatics* **10,** 421
31. Jain, E., Bairoch, A., Duvaud, S., Phan, I., Redaschi, N., Suzek, B. E., Martin, M. J., McGarvey, P., and Gasteiger, E. (2009) Infrastructure for the life sciences: design and implementation of the UniProt website. *BMC Bioinformatics* **10,** 136
32. Johnson, M., Zaretskaya, I., Raytselis, Y., Merezhuk, Y., McGinnis, S., and Madden, T. L. (2008) NCBI BLAST: a better web interface. *Nucleic Acids Res.* **36,** W5–9
33. Sheffield, P., Garrard, S., and Derewenda, Z. (1999) Overcoming expression and purification problems of RhoGDI using a family of "parallel" expression vectors. *Protein Expr. Purif.* **15,** 34–39
34. McCoy, A. J., Grosse-Kunstleve, R. W., Adams, P. D., Winn, M. D., Storoni, L. C., and Read, R. J. (2007) Phaser crystallographic software. *J. Appl. Crystallogr* **40,** 658–674
35. Zwart, P. H., Afonine, P. V., Grosse-Kunstleve, R. W., Hung, L. W., Ioerger, T. R., McCoy, A. J., McKee, E., Moriarty, N. W., Read, R. J., Sacchettini, J. C., Sauter, N. K., Storoni, L. C., Terwilliger, T. C., and Adams, P. D. (2008) Automated structure solution with the PHENIX suite. *Methods Mol. Biol.* **426,** 419–435
36. Collaborative Computational Project, Number 4 (1994) The CCP4 suite: programs for protein crystallography. *Acta Crystallogr. D Biol. Crystallogr.* **50,** 760–763
37. Arnold, K., Bordoli, L., Kopp, J., and Schwede, T. (2006) The SWISS-MODEL workspace: a web-based environment for protein structure ho-

mology modelling. *Bioinformatics* **22,** 195–201
38. Kiefer, F., Arnold, K., Künzli, M., Bordoli, L., and Schwede, T. (2009) The SWISS-MODEL Repository and associated resources. *Nucleic Acids Res.* **37,** D387–392
39. Vagin, A. A., Steiner, R. A., Lebedev, A. A., Potterton, L., McNicholas, S., Long, F., and Murshudov, G. N. (2004) REFMAC5 dictionary: organization of prior chemical knowledge and guidelines for its use. *Acta Crystallogr. D Biol. Crystallogr* **60,** 2184–2195
40. Morris, R. J., Perrakis, A., and Lamzin, V. S. (2003) ARP/wARP and automatic interpretation of protein electron density maps. *Methods Enzymol.* **374,** 229–244
41. Emsley, P., and Cowtan, K. (2004) COOT: model-building tools for molecular graphics. *Acta Crystallogr. D Biol. Crystallogr.* **60,** 2126–2132
42. Livnah, O., Bayer, E. A., Wilchek, M., and Sussman, J. L. (1993) The structure of the complex between avidin and the dye, 2-(4′-hydroxyazobenzene) benzoic acid (HABA). *FEBS Lett.* **328,** 165–168
43. Chivers, C. E., Koner, A. L., Lowe, E. D., and Howarth, M. (2011) How the biotin-streptavidin interaction was made even stronger: investigation via crystallography and a chimaeric tetramer. *Biochem. J.* **435,** 55–63
44. Teulon, J. M., Delcuze, Y., Odorico, M., Chen, S. W., Parot, P., and Pellequer, J. L. (2011) Single and multiple bonds in (strept)avidin-biotin interactions. *J. Mol. Recognit.* **24,** 490–502
45. González, M., Argaraña, C. E., and Fidelio, G. D. (1999) Extremely high thermal stability of streptavidin and avidin upon biotin binding. *Biomol. Eng.* **16,** 67–72
46. Chilkoti, A., Tan, P. H., and Stayton, P. S. (1995) Site-directed mutagenesis studies of the high affinity streptavidin-biotin complex: contributions of tryptophan residues 79, 108, and 120. *Proc. Natl. Acad. Sci. U.S.A.* **92,** 1754–1758
47. DeLano, W. L. (2010) *The PyMOL Molecular Graphics System*, version 1.3r1, Schrödinger, LLC, New York
48. Feller, G., and Gerday, C. (2003) Psychrophilic enzymes: hot topics in cold adaptation. *Nat. Rev. Microbiol.* **1,** 200–208
49. Casanueva, A., Tuffin, M., Cary, C., and Cowan, D. A. (2010) Molecular adaptations to psychrophily: the impact of "omic" technologies. *Trends Microbiol.* **18,** 374–381